



## NMR structure of human thymosin alpha-1

Miguel-Angel Elizondo-Riojas<sup>a,b</sup>, Steven M. Chamow<sup>c</sup>, Cynthia W. Tuthill<sup>d</sup>, David G. Gorenstein<sup>a</sup>, David E. Volk<sup>a,\*</sup>

<sup>a</sup> Center for Proteomics and Systems Biology, Institute of Molecular Medicine for the Prevention of Human Diseases, Department of NanoMedicine and Biomedical Engineering, University of Texas Health Science Center–Houston, 1825 Pressler, Houston, TX 77030, United States

<sup>b</sup> Centro Universitario Contra el Cáncer, Hospital Universitario "Dr. José Eleuterio González", Universidad Autónoma de Nuevo León, Monterrey, NL, Mexico

<sup>c</sup> S&J Chamow, Inc., Biopharmaceutical Consulting, San Mateo, CA 94403, United States

<sup>d</sup> SciClone Pharmaceuticals, Inc., 950 Tower Lane, Suite 900, Foster City, CA 94404, United States

### ARTICLE INFO

#### Article history:

Received 2 November 2011

Available online 15 November 2011

#### Keywords:

NMR data collection

Chemical shift assignment

Protein structure determination

Thymosin alpha1

Thymalfasin

Trifluoroethanol

### ABSTRACT

800 MHz NMR structure of the 28-residue peptide thymosin alpha-1 in 40% TFE/60% water (v/v) has been determined. Restrained molecular dynamic simulations with an explicit solvent box containing 40% TFE/60% TIP3P water (v/v) were used, in order to get the 3D model of the NMR structure. We found that the peptide adopts a structured conformation having two stable regions: an alpha-helix region from residues 14 to 26 and two double  $\beta$ -turns in the N-terminal twelve residues which form a distorted helical structure.

© 2011 Elsevier Inc. All rights reserved.

### 1. Introduction

Thymosin alpha-1 (thymalfasin) is an immunomodulating thymic peptide naturally produced by the thymus gland. It is approved for the treatment of several viruses and as an adjuvant for immunity enhancement. Recent studies have investigated the effects of thymosin alpha-1 and prothymosin alpha-1 on human cytomegalovirus [1], invasive Aspergillosis [2], dendritic cell tryptophan catabolism [3], HIV-1 [4,5], hepatitis B [6,7] and hepatitis C [8,9]. It is a hormone peptide created from a precursor protein, prothymosin, and is a 28-residue peptide that is acetate capped on the N-terminus.

### 2. Materials and methods

#### 2.1. NMR spectroscopy

A 28.8 mg sample of thymosin alpha-1 (Zadaxin, SciClone Pharma) was dissolved into 3.9 ml of 40% trifluoroethanol (TFE), 10% D<sub>2</sub>O and 50% H<sub>2</sub>O. The pH was adjusted to 4.9, and 30 s of centrifugation at 10,000 rpm provided a clear solution, which was decanted and placed into a Wilmad (541-PP-8) 5 mM NMR tube for data collection at 25 °C. A 300 ms 2D-NOESY and a 65 ms 2D-TOCSY were acquired on an 800 MHz Varian Unity+

spectrometer equipped with an RT probe with a 12.019 kHz spectral width and 2048 and 1024 complex data points F2 and F1, respectively. The NMR data were processed using Felix software (Felix, Inc.).

#### 2.2. Structure determination

##### 2.2.1. Initial structure

Both the pattern of NOE crosspeaks observed and initial unrestrained MD simulations starting from a linear peptide suggested the presence of an alpha-helix segment between residues 14 and 26, therefore an initial structure was built with three areas: (i) a linear structure from residues 1 to 14, (ii) an alpha-helix structure from residues 15 to 25 and (iii) a linear structure for the rest of the peptide. The N-terminal acetylation was also included into the model. The sequence of the modeled peptide is: (ACE)-Ser1-Asp-Ala-Ala-Val5-Asp-Thr-Ser-Ser-Glu10-Ile-Thr-Thr-Lys-Asp15-Leu-Lys-Glu-Lys-Lys20-Glu-Val-Val-Glu-Glu25-Ala-Glu-Asn28.

##### 2.2.2. Building a solvation box with 40% TFE/60% water

Before the peptide's solvation for unrestrained and restrained MD simulations took place, a unit box (without peptide) of approximately 90 × 90 × 90 Å<sup>3</sup> with 40% trifluoroethanol (TFE)/60% water (vol/vol; 1TFE:6H<sub>2</sub>O) was built containing 8618 TIP3P water model molecules and 1434 TFE molecules. The geometry and energy of the TFE molecule were initially optimized with Gaussian03 [10] using HF/6-31G\* level of theory and then a single-point calculation,

\* Corresponding author. Fax: +1 713 500 0319.

E-mail address: [David.Volk@uth.tmc.edu](mailto:David.Volk@uth.tmc.edu) (D.E. Volk).

with the same level of theory, was performed to obtain the electrostatic potential. Fitting charges to the electrostatic potential were then performed with RESP [11] obtaining the following charges for TFE atoms:  $F = -0.206066e$ ,  $C = 0.553137e$ ,  $CH_2 = (0.106937e + 2 \times 0.072737e) = 0.252411e$ ,  $OH = -0.616023e$  and  $HO = 0.428673e$  (where OH and HO are the hydroxylic oxygen and hydrogen atoms, respectively). Equal partial charges were given to equivalent atoms.

The 40% TFE/60% water box was minimized starting with 1000 steps with the steepest descent method then switched to 4000 steps of conjugate gradient or when the convergence criterion for the energy gradient was less than 0.01 kcal/mol Å. The system was then equilibrated following the next protocol: (i) 40 ps to gradually heat the system from 0 to 300 K keeping all molecules restrained by 25 kcal/mol Å<sup>2</sup> under NVT conditions, (ii) 20 ps at 300 K with all molecules restrained by 25 kcal/mol Å<sup>2</sup> under NVT conditions, (iii) the system was subsequently equilibrated in seven rounds over 380 ps where the positional restraints were gradually relaxed under NPT conditions and (iv) the production of 1 ns MD simulation at 300 K under NPT conditions was performed. This final equilibrated box was used as a solvation unit box during the peptide's solvation process within the xLeap program [11]. The long-range electrostatics were accounted for using the particle-mesh Ewald summation method, as implemented in the PMEMD module of AMBER9 and a combined force field "GAFF + ff99SB" was applied. The SHAKE algorithm [12] was used to constrain covalent bonds to hydrogen atoms allowing a time step of 2 fs. A cutoff of 9 Å was chosen for the non-bonded van der Waals interactions. During the heating protocol at NVT conditions, the Berendsen temperature coupling algorithm [13] was used with a coupling constant of 2.0 ps. During the equilibration and production of the simulation, the Langevin dynamics were used with a collision frequency of 1.0 ps<sup>-1</sup>.

### 2.2.3. MD simulations

**2.2.3.1. 25 ns unrestrained MD simulation at 300 K on 40% TFE/60% water solvent.** The initial structure (see Initial structure section) was neutralized adding 6Na<sup>+</sup> counterions using an algorithm of xLeap [11]. The latter structure was then surrounded by a 10 Å layer of pre-equilibrated 40% TFE/60% TIP3P solvation unit box (see Section 2.2.2) in an orthorhombic box of approximately 60 × 90 × 60 Å<sup>3</sup> containing a total of 16,737 atoms. The system was minimized by 1000 steps steepest descent method then 4000 steps of conjugate gradient or when the energy gradient was less than 0.01 kcal/mol Å. The solvated system was then equilibrated following the same protocol as given above (see Section 2.2.2) except that the system was equilibrated in seven rounds over 380 ps where the positional restraints were gradually relaxed until the solvent and counterions were free to move while restraining the solute (2 kcal/mol Å<sup>2</sup>) under NPT conditions. The solute was finally relaxed in seven rounds over 3.5 ns as positional restraints were gradually removed. A production phase followed with 25 ns unrestrained MD simulation at 300 K under NPT condition. Structure snapshots were collected every 1 ps.

**2.2.3.2. 1 ns restrained MD simulation at 300 K on implicit solvent.** The last structure of the latter 25 ns unrestrained MD simulation was used as the initial structure for a restrained MD simulation on implicit solvent using the Generalized Born method [14] at 300 K. The idea of this simulation was to find a good initial structure (low NMR restraints penalty) for a final restrained MD simulation on 40% TFE/60% TIP3P explicit solvent during 10 ns (see next section). In order to find a good structure with low NMR penalty for the 549 restraints applied, we followed this protocol: (i) 100 ps to gradually heat the system from 0 to 300 K keeping all residues restrained by 25 kcal/mol Å<sup>2</sup>, (ii) the system was then equilibrated in three rounds over 120 ps where the

positional restraints were gradually removed leaving a stable system at 300 K, (iii) during the next 400 ps all NMR restraints energy terms were proportionally increased from 0% to 200% of its default values, (iv) then a 200 ps simulation followed where all NMR restraints energy terms were proportionally decreased from 200% to 100%, and (v) 400 ps where all NMR restraints energy terms were kept at 100%, (vi) from this last period one stable structure was selected followed by 1 ns restrained MD simulation on implicit solvent at 300 K with all (549) NMR restraints applied. 1000 structure snapshots were collected. The Generalized Born method (ig = 5) was employed and the force field "ff99SB" implemented in AMBER9 [11] was applied. The SHAKE algorithm [12] was used to constrain covalent bonds to hydrogen atoms and a time step of 1 fs was used. No cutoff was used for the long-range interactions. During the heating protocol, the Berendsen temperature coupling algorithm [13] was employed with a coupling constant of 0.8 ps. During the equilibration and production of the simulation, the Langevin dynamics was used with a collision frequency of 1.0 ps<sup>-1</sup>. The 1000 collected structures were then minimized with the Generalized Born method (ig = 5) including all NMR restraints (549) starting with 500 steps with the steepest descent method then switched to 500 steps of conjugate gradient or when the convergence criterion for the energy gradient was less than 0.01 kcal/mol Å, and finally the 1000 structures were sorted by energy. The lowest energy structure was then selected for the next and last simulation.

**2.2.3.3. 10 ns restrained MD simulation at 300 K on 40% TFE/60% water solvent.** The lowest energy structure from the previous MD simulation was used as initial structure for a 10 ns NMR restrained MD simulation at 300 K in 40% TFE/60% water solvent. The initial structure neutralized with 6Na<sup>+</sup> counterions was surrounded by a 10 Å layer of pre-equilibrated 40% TFE/60% TIP3P solvation unit box (see Section 2.2.2) in an orthorhombic box of approximately 60 × 45 × 60 Å<sup>3</sup> containing a total of 8088 atoms. The system was minimized starting with 1000 steps with the steepest descent method then switched to 4000 steps of conjugate gradient or when the convergence criterion for the energy gradient was less than 0.01 kcal/mol Å. The solvated system was then equilibrated following the same protocol as given above (see Section 2.2.2) except that after the step (iii) where the system was equilibrated in seven rounds over 380 ps and the positional restraints were gradually relaxed at 300 K under NPT condition, the equilibration followed the next protocol: (iv) during the next 500 ps all NMR restraints energy terms were proportionally increased from 0% to 200% of its default values, (v) followed by 300 ps where all NMR restraints energy terms were proportionally decreased from 200% to 100% and finally, (vi) a production of 10 ns restrained MD simulation at 300 K under NPT condition with all NMR restraints was performed. During the last nanosecond one thousand structures were collected, then minimized with the Generalized Born method (ig = 5) including all NMR restraints (549) starting with 1000 steps with the steepest descent method then switched to 1000 steps of conjugate gradient or when the convergence criterion for the energy gradient was less than 0.01 kcal/mol Å, and finally the 1000 structures were sorted by energy. The best 20 structures with the lowest energy were selected. The average structure was obtained from the average of the 20 best structures and then minimized.

## 3. Results

### 3.1. Chemical shift assignments

Following well-established methods [15], the TOCSY correlations were used to create a list of amino acid spin system

assignments, as denoted by horizontal lines in Fig. 1. Data provided complete spin system assignments by correlations between the side chain protons with H $\alpha$  (Fig. 1A) or HN (Fig. 1B). Assignment of the initial group of spin systems into specific peptide positions was based on sequential and medium-range correlations observed in the 2D NOESY spectrum. The HN–HN region of the NOESY

spectrum provided many strong sequential correlations (Fig. 1C). Sequential HN–HN correlations from residues 1 to 11 and from residues 13 to 28 are shown. Residues 11–13 have nearly identical HN values making this region less useful for their assignments. The present assignments (Table 1) represent a comprehensive proton resonance list.

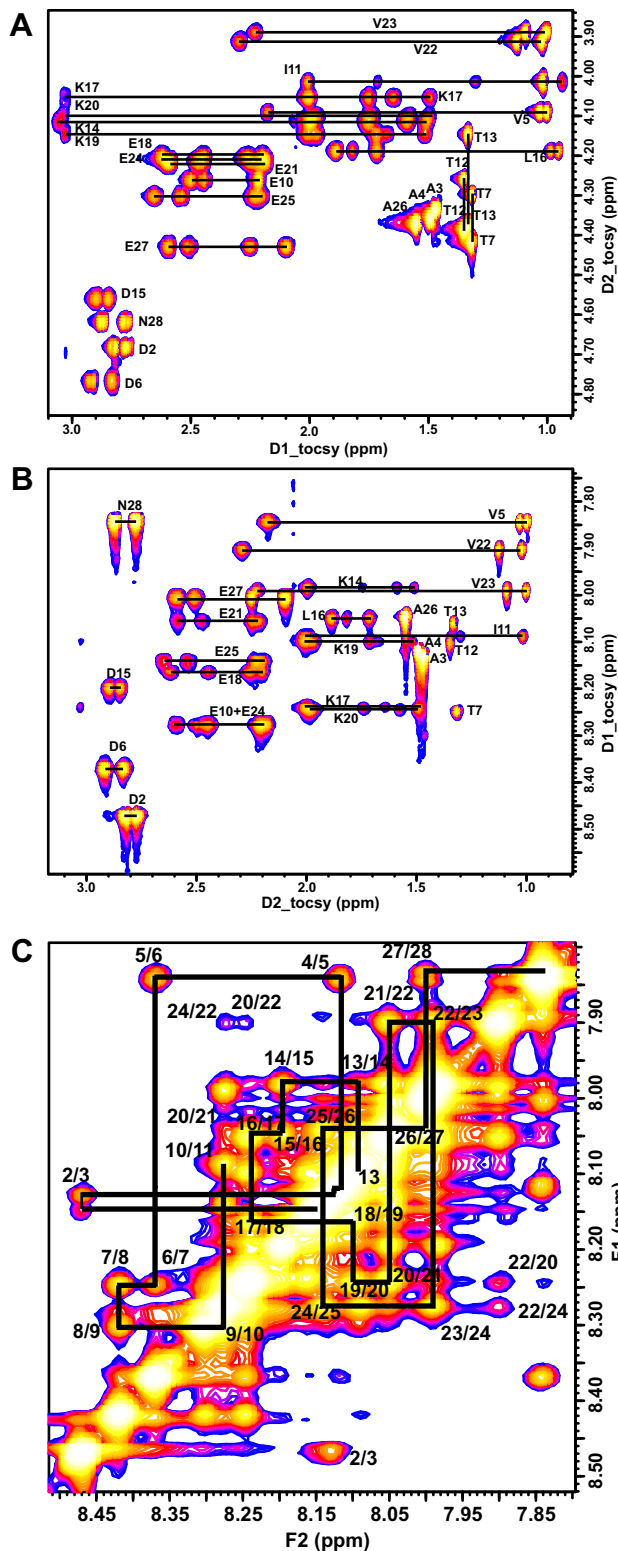


**Fig. 1.** Experimental 2D TOCSY (A, B) and NOESY (C) spectra for thymosin alpha-1 in 40% TFE/60% water (v/v) solution. Sequential correlation assignments of the NOE cross peaks are indicated in panel C.

### 3.2. Structural statistics of the 20 best structures

During the restrained MD simulations and energy minimizations 549 restraints were applied. A total of 415 NOE restraints accounting for: 170 intra-residue, 139 sequential ( $|i - j| = 1$ ), 106 medium range ( $1 < |i - j| < 5$ ), and 0 long range ( $|i - j| > 5$ ) restraints. One hundred constraints for chirality and planarity were used and, based on preliminary MD simulations and NOE patterns, 17 dihedral angle restraints for phi and psi angles for residues 11–27 were also applied. From the ensemble of 20 lowest energy structures we found that the average distance violation was  $0.0086 \pm 0.036 \text{ \AA}$  and the average torsion angle violation was  $0.0719 \pm 0.4223^\circ$ . The backbone atom superposition of the 20 lowest energy structures fitted to residues 1–11 (Fig. 2A) has a rmsd to average structure of  $0.35 \pm 0.08 \text{ \AA}$  and when fitted to residues 12–28 (Fig. 2B) the backbone atom superposition has a rmsd to average structure of  $0.38 \pm 0.09 \text{ \AA}$ . A stereoview representation of the average structure is shown in Fig. 2C.

### 3.3. Structure analysis

The peptide has a stable C-terminal alpha-helix segment between residues 14 and 26 and also a stable distorted helical structure for the N-terminal residues 1–12. The flexibility between these two stable regions can be observed in Fig. 2A and B and also in Fig. 3 where the sequential and medium range NOEs connectivities are shown. From the 1000 structures collected on the last MD simulation (where the 20 lowest energy structures were found), we measure the distances between residues  $i$  and  $i + 3$  and the angles phi/psi for residues  $i + 1$  and  $i + 2$  over the residues 1–14, and we found two double  $\beta$ -turns. An (I,I + 1)-double turn is present

**Table 1**  
Chemical shift assignments of thymosin alpha-1.

Residue	HN	H $\alpha$	H $\beta$	Others
Ser 1	8.150	4.487	3.987, 3.892	
Asp 2	8.471	4.680	2.823, 2.770	
Ala 3	8.127	4.335	1.468	
Ala 4	8.112	4.358	1.490	
Val 5	7.840	4.090	2.173	1.030, 1.000
Asp 6	8.370	4.766	2.916, 2.829	
Thr 7	8.248	4.300	4.420	1.316
Ser 8	8.420	4.380	4.07, 4.04	
Ser 9	8.300	4.440	4.06, 4.00	
Glu 10	8.278	4.260	2.205	2.498, 2.444
Ile 11	8.090	4.013	2.003	1.710, 1.298, 1.018, 0.938
Thr 12	8.101	4.260	4.390	1.348
Thr 13	8.059	4.150	4.370	1.332
Lys 14	7.983	4.115	1.990	1.59, 1.51, 1.74, 3.05
Asp 15	8.197	4.559	2.89, 2.85	
Leu 16	8.046	4.187	1.883, 1.714	1.817, 0.984, 0.951
Lys 17	8.240	4.054	2.000	1.49, 1.75, 1.64, 3.03
Glu 18	8.164	4.201	2.259, 2.199	2.615, 2.443
Lys 19	8.096	4.144	2.007, 1.970	1.513, 1.334, 1.717, 1.675, 3.03
Lys 20	8.244	4.102	2.22, 1.99	1.59, 1.49, 1.96, 1.74, 3.02
Glu 21	8.054	4.214	2.245, 2.218	2.582, 2.470
Val 22	7.899	3.910	2.289	1.127, 1.020
Val 23	7.987	3.890	2.222	1.090, 1.004
Glu 24	8.273	4.210	2.25, 2.19	2.59, 2.47
Glu 25	8.139	4.302	2.224, 2.197	2.648, 2.537
Ala 26	8.043	4.370	1.550	
Glu 27	8.005	4.428	2.25, 2.10	2.59, 2.51
Asn 28	7.842	4.620	2.87, 2.77	6.76, 7.58

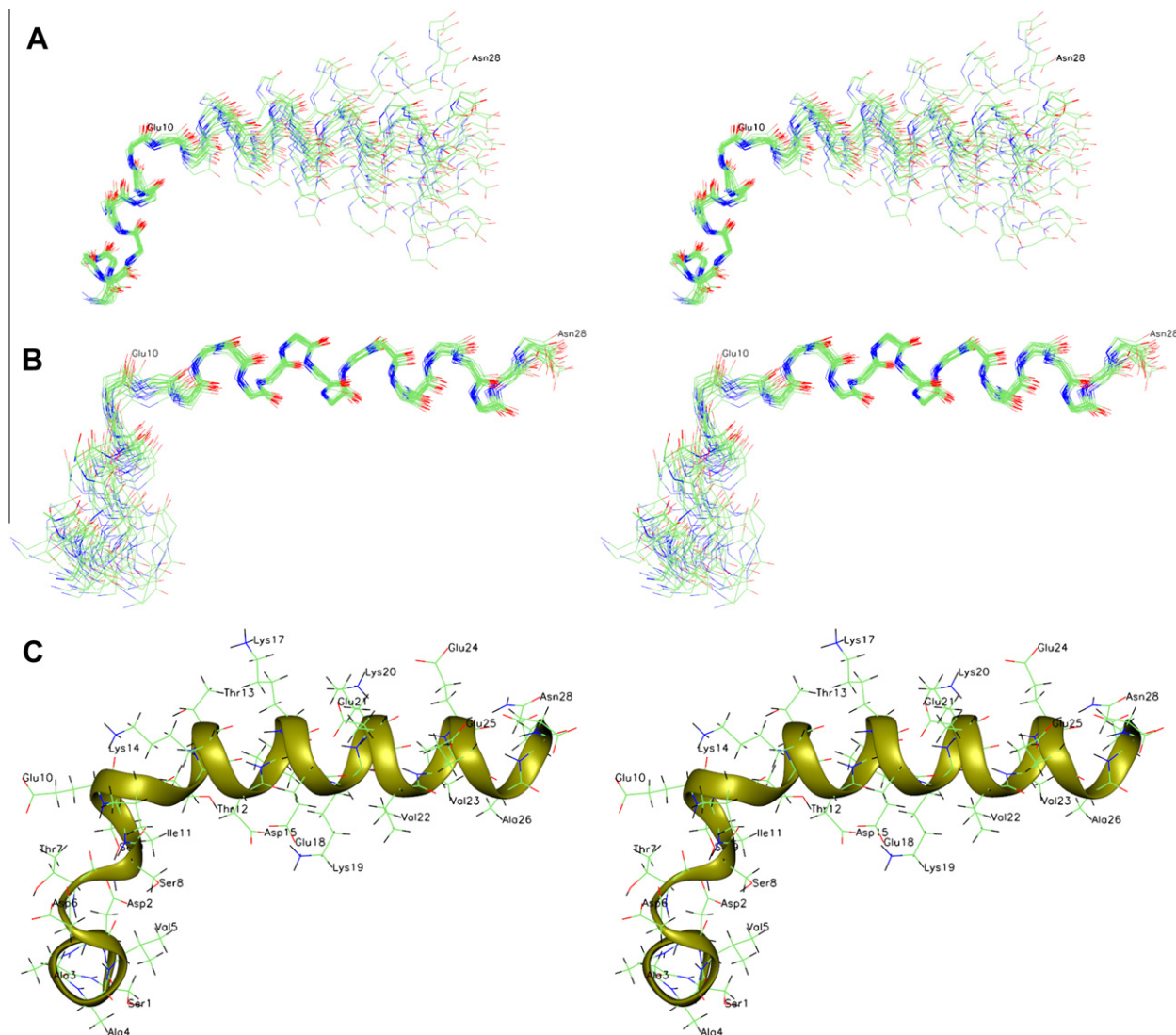


**Fig. 2.** Stereoviews of the final 20 lowest energy structures of thymosin alpha-1 in 40% TFE/60% water (v/v) solution. Backbone superposition aligned for (A) N-terminal region fitted to residues 1–11 and (B) C-terminal region fitted to residues 12–28. Ribbon/lines stereoview representation of the average structure of the 20 lowest energy structures is shown in (C). Pictures produced using VMD program [18].

from residues Asp2–Asp6 and an (I,I+2) double turn is present from residues Thr7–Thr12. The four type-I  $\beta$ -turns within these two double turns are [16] characterized as follows: (A) Asp2–Ala3–Ala4–Val5,  $\text{dist}(i, i+3) = 5.0 \pm 0.2 \text{ \AA}$ ,  $\text{phi}/\text{psi}(i+1) = -64.1 \pm 8.3^\circ / -32.5 \pm 9.5^\circ$ ,  $\text{phi}/\text{psi}(i+2) = -72.3 \pm 10.8^\circ / -14.1 \pm 13.1^\circ$ ; (B) Ala3–Ala4–Val5–Asp6,  $\text{dist}(i, i+3) = 4.9 \pm 0.3 \text{ \AA}$ ,  $\text{phi}/\text{psi}(i+1) = -72.3 \pm 10.8^\circ / -14.1 \pm 13.1^\circ$ ,  $\text{phi}/\text{psi}(i+2) = -105.7 \pm 15.5^\circ / 14.9 \pm 8.8^\circ$ ; (C) Thr7–Ser8–Ser9–Glu10,  $\text{dist}(i, i+3) = 6.3 \pm 0.4 \text{ \AA}$ ,  $\text{phi}/\text{psi}(i+1) = -65.6 \pm 10.6^\circ / -17.9 \pm 9.1^\circ$ ,  $\text{phi}/\text{psi}(i+2) = -59.6 \pm 8.9^\circ / -16.8 \pm 10.0^\circ$  and (D) Ser9–Glu10–Ile11–Thr12,  $\text{dist}(i, i+3) = 5.7 \pm 0.4 \text{ \AA}$ ,  $\text{phi}/\text{psi}(i+1) = -86.9 \pm 12.9^\circ / -36.8 \pm 12.6^\circ$ ,  $\text{phi}/\text{psi}(i+2) = -86.5 \pm 6.7^\circ / -17.5 \pm 5.3^\circ$ .

#### 4. Discussion

Although the present NMR assignments for thymosin alpha-1 reported (Table 1; BioMagResBank Accession ID: 17458) generally agreed to within about 0.1 ppm with those previously reported [17], a significant number of shifts show larger differences. The present assignments include the Ile11, Leu16, Glu25, Glu27 and Asn28 amide protons which were missing in the previous work,

as well as the complete side chain assignments for Glu25, Glu27 and Asn28 which were previously not assigned. Of particular note, our assignments for the Ile11 and Leu16 alpha protons, 4.013 and 4.187 ppm, differ greatly from the earlier report which listed them as 3.01 and 3.11 ppm, respectively. The previous Ile11  $H_\alpha$  value appears to have been an incorrect assignment of Lys19  $H_\alpha$  to Ile11  $H_\alpha$ , due to resonance overlap not resolvable on a 400 MHz magnet. The present assignments are complete.

The 800 MHz NMR structure determination of the 28-residue peptide thymosin alpha-1 in 40% TFE/60% water (v/v) solution shows that the peptide adopts a structured conformation having two stable regions: an alpha-helix region from residues 14 to 26 and two double  $\beta$ -turns in the N-terminal twelve residues which form a distorted helical structure. The (I,I+1) double turn is formed by type-I  $\beta$ -turn Asp2–Ala3–Ala4–Val5 and Ala3–Ala4–Val5–Asp6. The (I,I+2) double turn is formed by type-I  $\beta$ -turns Thr7–Ser8–Ser9–Glu10 and Ser9–Glu10–Ile11–Thr12. A 25 ns unrestrained MD simulation followed by a 10 ns NMR restrained MD simulation at 300 K on 40% TFE/60% TIP3P water model solvent were used to obtain the 3D structure of the 28-residue peptide of thymosin alpha-1 (PDB ID: 219i).

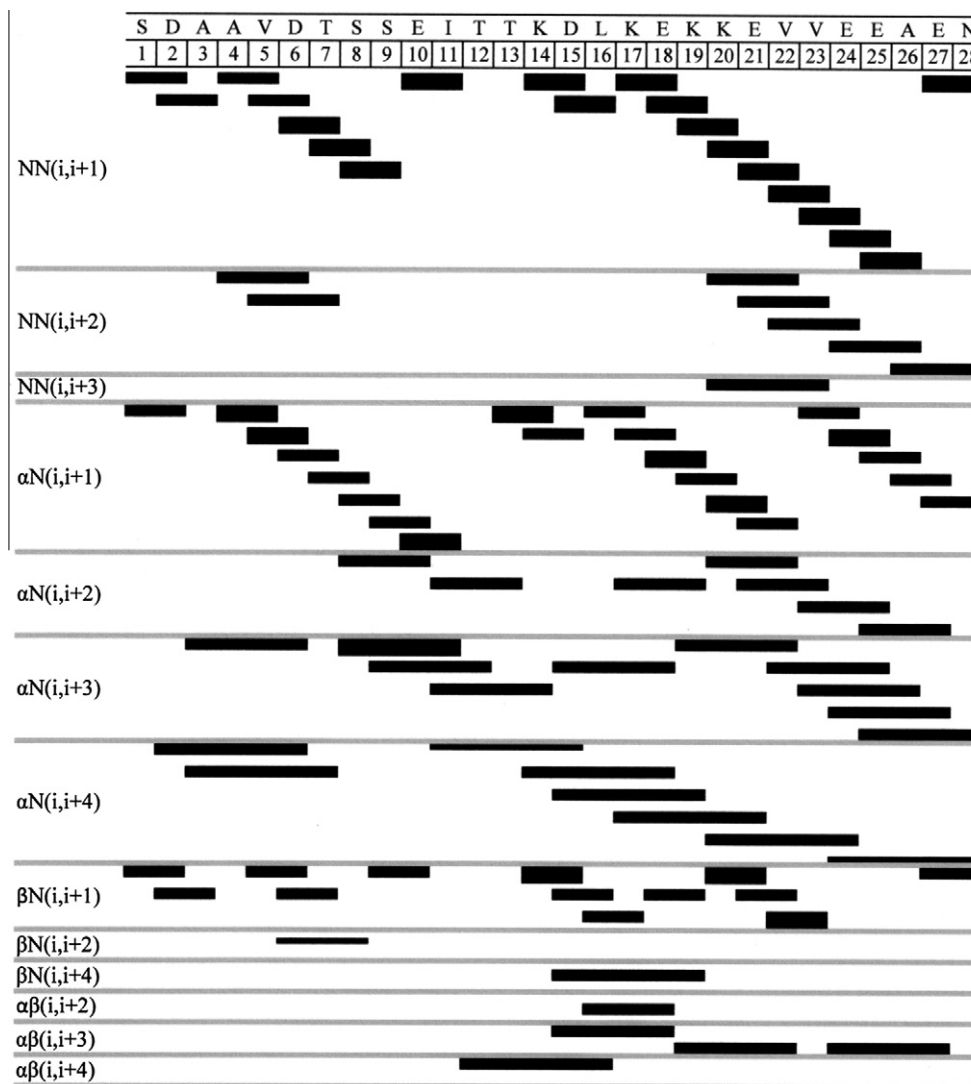


**Fig. 3.** Summary of sequential and medium range NOEs connectivities of thymosin alpha-1 in 40% TFE/60% water (v/v) solution. The thicknesses of the lines represent the intensity of NOE cross peaks classified as strong, medium and weak.

### Acknowledgments

The authors would like to thank the W.M. Keck Foundation and the John S. Dunn, Sr. Foundation for supporting the John S. Dunn, Sr. Gulf Coast Consortium for Magnetic Resonance which purchased the 800 MHz NMR spectrometer used in these studies and Sean Moran at Rice University for assistance with NMR data collection. This work was funded by a grant from SciClone Pharmaceutical, which also kindly provided the thymosin-alpha1.

### References

- [1] S. Bozza, P. Bonifazi, T. Zelante, et al., Thymosin alpha1 activates the TLR9/MyD88/IRF7-dependent murine cytomegalovirus sensing for induction of antiviral responses in vivo, *Int. Immunol.* 19 (2007) 1261–1270.
- [2] B.H. Segal, T.J. Walsh, Current approaches to diagnosis and treatment of invasive aspergillosis, *Am. J. Respir. Crit. Care Med.* 173 (2006) 707–717.
- [3] L. Romani, F. Bistoni, K. Perruccio, C. Montagnoli, R. Gaziano, et al., Thymosin alpha1 activates dendritic cell tryptophan catabolism and establishes a regulatory environment for balance of inflammation and tolerance, *Blood* 108 (2006) 2265–2274.
- [4] A. Mosoian, A. Teixeira, et al., Novel function of prothymosin alpha as a potent inhibitor of human immunodeficiency virus type 1 gene expression in primary macrophages, *J. Virol.* 80 (2006) 9200–9206.
- [5] A. Mosoian, A. Teixeira, et al., Prothymosin-alpha inhibits HIV-1 via Toll-like receptor 4-mediated type I interferon induction, *PNAS* 107 (2010) 10178–10183.
- [6] S. Iino, J. Toyota, H. Kumada, et al., The efficacy and safety of thymosin alpha-1 in Japanese patients with chronic hepatitis B; results from a randomized clinical trial, *J. Viral Hepat.* 12 (2005) 300–306.
- [7] J. You, L. Zhuang, H.-Y. Cheng, et al., Efficacy of thymosin alpha-1 and interferon alpha in treatment of chronic viral hepatitis B: a randomized controlled study, *World J. Gastroenterol.* 12 (2006) 715–721.
- [8] P. Andreone, C. Cursaro, A. Gramenzi, et al., In vitro effect of thymosin-alpha1 and interferon-alpha on Th1 and Th2 cytokine synthesis in patients with chronic hepatitis C, *J. Viral Hepat.* 8 (2001) 194–201.
- [9] P. Kullavanuava, S. Treeprasertsuk, D. Thong-Ngam, K. Chaermtai, S. Gonlakanvit, P. Suwanagool, The combined treatment of interferon alpha-2a and thymosin alpha 1 for chronic hepatitis C: the 48 weeks end of treatment results, *J. Med. Assoc. Thai.* 84 (2001) 462–468.
- [10] M.J. Frisch, G.W. Trucks, H.B. Schlegel, G.E. Scuseria, M.A. Robb, J.R. Cheeseman, J.A. Montgomery Jr., T. Vreven, et al., GAUSSIAN 03, Revision B.05, Gaussian Inc., Wallingford CT, 2004.
- [11] D.A. Case, T.A. Darden, T.E. Cheatham III, C.L. Simmerling, J. Wang, R.E. Duke, R. Luo, K.M. Merz, D.A. Pearlman, M. Crowley, R.C. Walker, W. Zhang, B. Wang, S. Hayik, A. Roitberg, G. Seabra, K.F. Wong, F. Paesani, X. Wu, S. Brozell, V. Tsui, H. Gohlke, L. Yang, C. Tan, J. Mongan, V. Hornak, G. Cui, P. Beroza, D.H. Mathews, C. Schafmeister, W.S. Ross, P.A. Kollman, AMBER 9, University of California, San Francisco, 2006.
- [12] J.P. Ryckaert, G. Ciccotti, H.J.C. Berendsen, Numerical integration of the Cartesian equations of motion of a system with constraints: molecular dynamics of *n*-alkanes, *J. Comput. Phys.* 23 (1977) 327–341.

- [13] H.J.C. Berendsen, J.P.M. Postma, W.F.V. Gunsteren, A. Dinola, J.R. Haak, Molecular dynamics with coupling to an external bath, *J. Chem. Phys.* 81 (1984) 3684–3690.
- [14] V. Tsui, D.A. Case, Theory and applications of the generalized Born solvation model in macromolecular simulations, *Biopolymers* 56 (2001) 275–291.
- [15] K. Wüthrich, *NMR of Proteins and Nucleic Acids*, John Wiley and Sons, New York, 1986.
- [16] E.G. Hutchinson, J.M. Thornton, A revised set of potentials for beta turn formation in proteins, *Protein Sci.* 3 (1994) 2207–2216.
- [17] A. Grottesi, M. Sette, T. Palamara, G. Rotilio, E. Garaci, M. Paci, The conformation of peptide thymosin alpha 1 in solution and in a membrane-like environment by circular dichroism and NMR spectroscopy. A possible model for its interaction with the lymphocyte membrane, *Peptides* 19 (1998) 1731–1738.
- [18] W. Humphrey, A. Dalke, K. Schulten, VMD – visual molecular dynamics, *J. Mol. Graphics* 14 (1996) 33–38.